IEEE Photonics Journal
An IEEE Photonics Society Publication

Generation and Propagation of Bound-State Pulses in a Passively Mode-Locked Figure-Eight Laser

Volume 4, Number 2, April 2012

Ling Yun
Xueming Liu, Member, IEEE

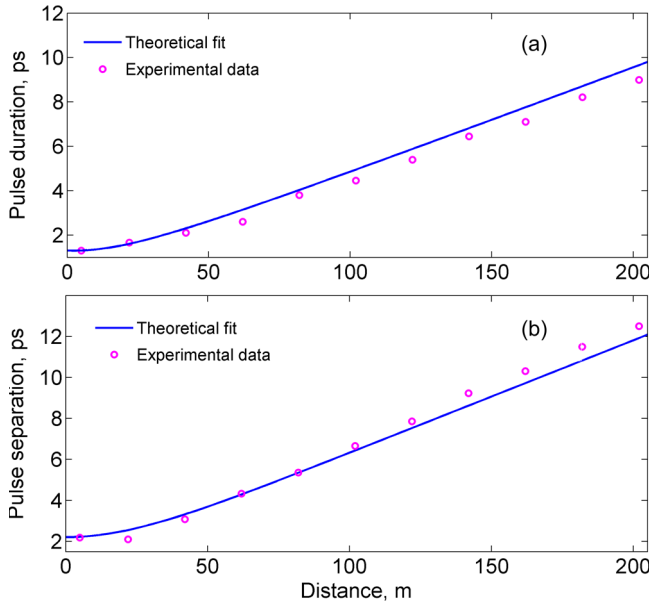

DOI: 10.1109/JPHOT.2012.2191948
1943-0655/$31.00 ©2012 IEEE

Generation and Propagation of Bound-State Pulses in a Passively Mode-Locked Figure-Eight Laser

Ling Yun and Xueming Liu, *Member, IEEE*

State Key Laboratory of Transient Optics and Photonics, Xi'an Institute of Optics and Precision Mechanics, Chinese Academy of Sciences, Xi'an 710119, China

DOI: 10.1109/JPHOT.2012.2191948
1943-0655/$31.00 ©2012 IEEE

Manuscript received February 24, 2012; revised March 18, 2012; accepted March 19, 2012. Date of current version April 6, 2012. This work was supported by the "Hundreds of Talents Programs" of the Chinese Academy of Sciences and by the National Natural Science Foundation of China under Grant 10874239 and Grant 10604066. Corresponding author: X. Liu (e-mail: liuxueming72@yahoo.com).

Abstract: We have investigated the generation and propagation of robust bound-state pulses emitted from a passively mode-locked figure-eight laser with net-anomalous dispersion. Two pulses with the pulse duration of ~1.3 ps and the separation of ~2.2 ps exhibit a strongly modulated spectral profile. The experimental observations show that the pulse duration and the separation increase approximately linearly along the extracavity single-mode fiber (SMF). The pulse duration and separation are broadened by a factor of ~7 and ~5.7, respectively, after the pulse pair propagates through the standard SMF of 202 m. The theoretical results well agree with the experimental observations.

Index Terms: Fiber optics systems, erbium lasers, ultrashort pulse, pulse propagation.

1. Introduction

The fiber-based continuous wave lasers or pulse lasers are very important on optical communication [1], [2]. Especially, solitons based on fiber lasers offer a platform of building new types of mode-locking lasers [3]–[11]. The mode-locking fiber lasers have become a platform for exhibiting various nonlinear phenomena, including the formation of soliton rain [4], dissipative solitons [5]–[14], harmonic solitons [15], vector solitons [16], [17], and bound-state pulses [18]–[21], as well as the dissipative soliton resonance [6], [22], [23] (or wave-breaking-free pulses [3], [7], [24]). In previous works, bound states have become an attractive topic in nonlinear optical fiber systems in both theoretical and experimental fields [25]–[31]. Depending on the formation mechanisms, bound states can be divided into two main types [9]. For the first type of long-range pulse interaction, the tails of the adjacent pulses do not overlap, and thus, direct pulse interaction can be ignored [31]. In some reports, the dispersive waves resulting from the periodic perturbations in the laser cavity play an essential role among the bound-state pulses with the large time separation [29]. The other type is equivalent fast saturable absorbers with short-range pulse interaction [27]. They are typically modeled by the coupled nonlinear Schrödinger equations or quintic complex Ginzburg–Landau equation. The formation of these bound-state pulses is due to direct interaction between the pulses [32], [33]. Usually such bound states consist of two pulses and are characterized by the peak-to-peak separation and the phase difference between the two pulses [31], [34].

Ortaç *et al.* had experimentally observed the high-power ultrashort bound states in an ytterbium-doped double-clad fiber laser mode-locked by nonlinear polarization rotation technique [26], where the laser generated chirped bound states of three pulses with either equal or different time

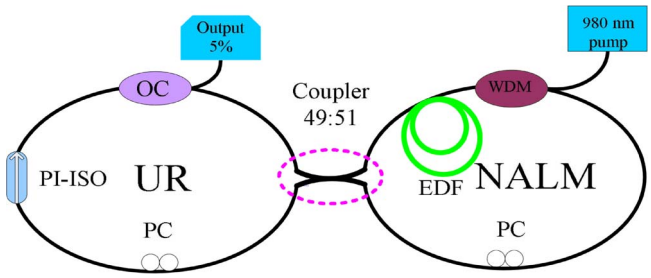

Fig. 1. Experimental setup of the figure-eight fiber laser. NALM: nonlinear amplifying loop mirror; UR: unidirectional ring; WDM: wavelength division multiplexer; PC: polarization controller; PI-ISO: polarization-insensitive isolator; OC: optical coupler; EDF: erbium-doped fiber.

separations. Hsiang *et al.* demonstrated the first experimental observation of stable bound soliton pairs at 10-GHz repetition rate in a hybrid frequency modulation harmonic mode-locked erbium-doped fiber (EDF) laser. The time separation between the two solitons in the pair was about three times the full-width at half-maximum (FWHM) of the soliton duration and varied with the phase modulation strength [19]. The robust dissipative soliton molecules with the pulse duration T_0 of about 20 ps and a peak-to-peak separation of about $8T_0$ were reported in the large normal path-averaged dispersion fiber lasers [25].

In our previous reports based on the nonlinear polarization rotation technique, the theoretical and experimental results show that pulses do not form the bound state and the pulse separation is more than an order of magnitude of the pulse duration in the ultralong anomalous-dispersion fiber lasers [13], [14]. In this paper, we report what is, to our knowledge, the first experimental observation of both the generation of stable bound-state pulses in a passively mode-locked figure-eight laser and their propagation passing through extracavity single-mode fiber (SMF). The two pulses have identical pulse shape with the pulse duration of $\sim$1.3 ps and the peak-to-peak separation of $\sim$2.2 ps. In addition, we demonstrate that both the pulse duration and the separation increase almost linearly with the propagation distance. Numerical simulations further confirm the experimental observations.

2. Experimental Setup

The laser used in our experiments is schematically shown in Fig. 1. It is an all-fiber figure-eight laser based on a passive unidirectional ring (UR) cavity that is coupled to a nonlinear amplifying loop mirror (NALM) through a 49/51 fiber coupler. The NALM contains a 12-m-long EDF (CorActive C300) with an absorption of 3 dB/m at 980 nm served as the gain medium, a wavelength division multiplexer (WDM), a polarization controller (PC), and a 7-m-long SMF. The UR is composed of a 95/5 fused optical coupler (OC), a polarization insensitive isolator (PI-ISO), and a PC. A 980-nm laser diode with the maximum pump power of 550 mW is used to provide pump source through a 980/1550 nm WDM. All other fibers in the cavity are standard SMF with the length of about 12 m. The dispersion parameter D for EDF and SMF are about -9 ps/nm/km and 17 ps/nm/km at 1550 nm, respectively. The net cavity dispersion is estimated to be about -0.12 ps^2. The total length of the figure-eight laser is $\sim$24 m, corresponding to the fundamental repetition rate of $\sim$8.4 MHz. For an input pulse of the proper intensity, the asymmetrically located amplifier induces a relative nonlinear phase shift between the pulses within the loop mirror. When the pulses interfere at the central 49:51 coupler, the high-intensity portions of the pulse are amplified and transmitted while the low-intensity portions are reflected and rejected by the optical isolator. In this way, the combination of the NALM and isolator acts as an equivalent saturable absorber. Mode locking can be obtained by the adjustment of the two PCs and with enough pump power and proper length of the NALM. The output is monitored with a high-speed photodetector and visualized with a 6-GHz oscilloscope (LeCroy SDA 8600A), the spectral properties are analyzed with an optical spectrum analyzer, the radio frequency spectrum is probed by a radio-frequency analyzer, and the pulse duration is measured with an autocorrelator.

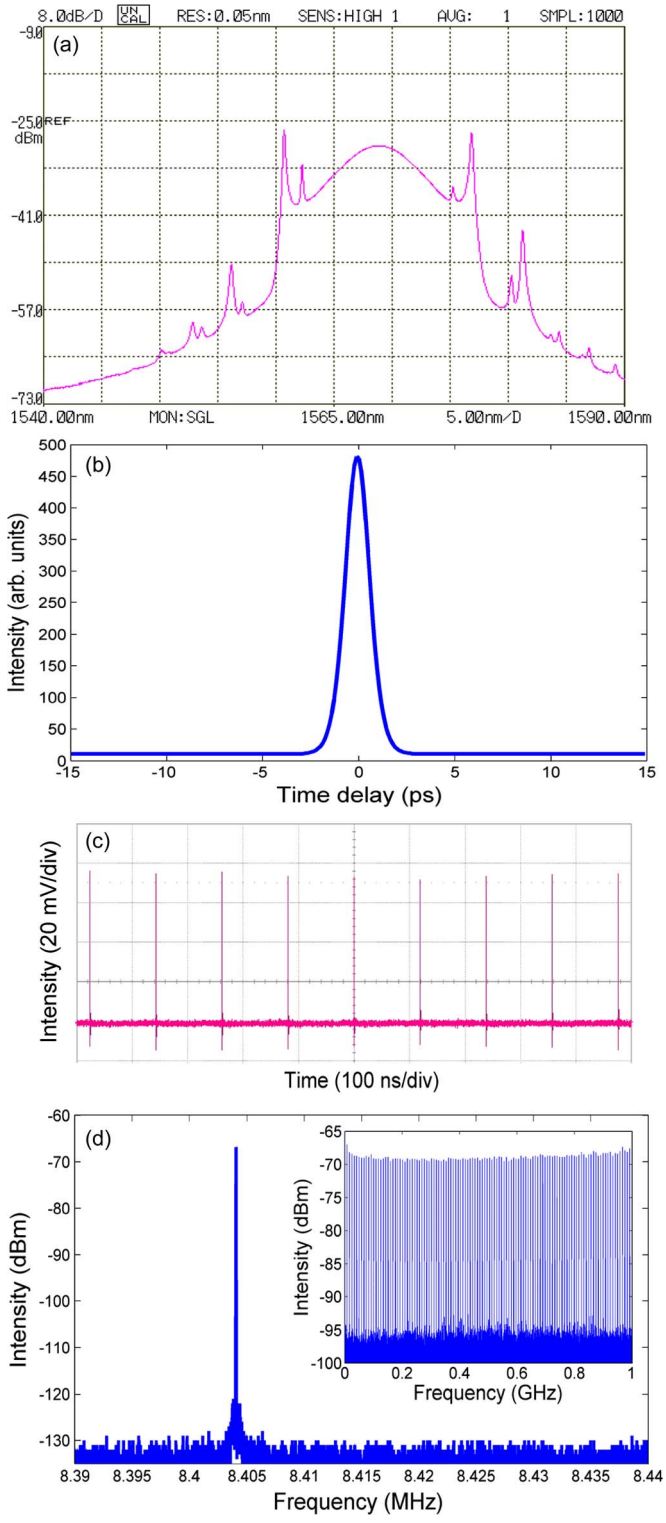

Fig. 2. Typical single-pulse soliton. (a) Optical spectrum, (b) autocorrelation trace, (c) oscilloscope trace, and (d) radio-frequency spectrum.

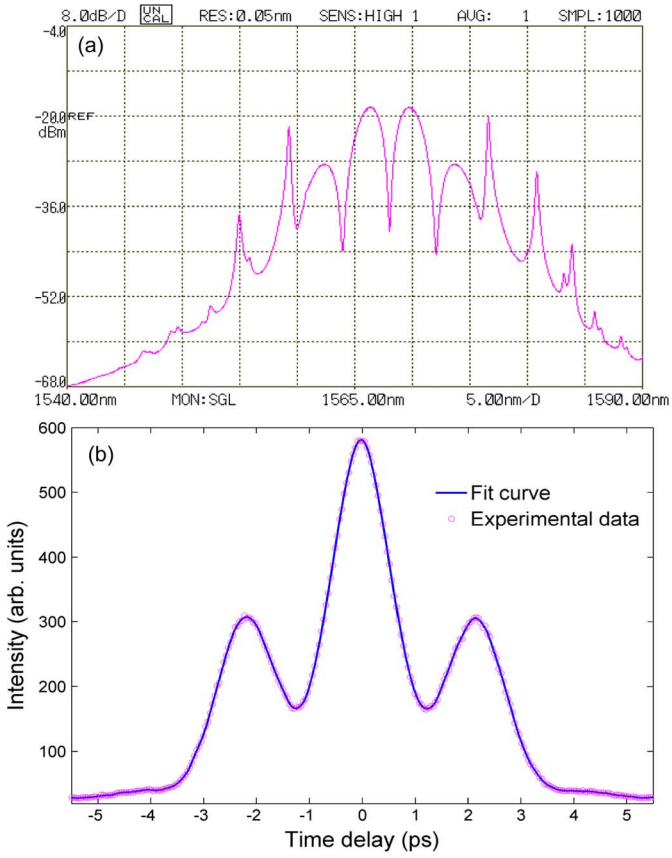

Fig. 3. Typical bound-state operation of the laser. (a) Spectrum and (b) autocorrelation trace.

3. Experimental Results and Analysis

With proper adjustment of the PCs, self-started mode locking of the fiber laser can be achieved above the mode-locking threshold. Mode-locked operation is characterized by the simultaneous generation of multiple pulses in the cavity. Then, the pump strength can be reduced to a value which is much lower than the mode-locking threshold, while still maintaining the pulse operation. Below this value, mode locking cannot be established and optical pulse suddenly disappears and turns to the continuous wave operation, which can be regarded as the hysteresis phenomenon [31], [33]. Fig. 2(a)–(d) show an example of single pulse operation at the pump power $P = 9$ mW. The central wavelength of optical spectrum is 1567 nm and the 3-dB spectral width is $\sim$5.4 nm, as shown in Fig. 2(a). The FWHM of the autocorrelation trace is $\sim$1.3 ps if the Gaussian pulse profile is assumed, as shown in Fig. 2(b). Thus, the time-bandwidth-product of the pulse is $\sim$0.88, indicating that the pulse is chirped. Fig. 3(c) shows the equally spaced pulses in the laser cavity, and each of them exhibits the same intensity in the oscilloscope. The spacing between the pulses is 120 ns, corresponding to the fundamental repetition rate of 8.4 MHz in radio-frequency analyzer. Fig. 2(d) shows the RF spectrum with a 10-Hz resolution bandwidth for the dual-wavelength mode-locked operation. The supermode suppression ratio is larger than 70 dB.

Fig. 3 shows the situation for the pump power P of 38 mW. The spectrum of the bound-state pulses shown in Fig. 3(a) is strongly modulated, which is a direct consequence of very close pulse separation in the temporal domain according to the Fourier transform (FT) theory [31]. The spectral modulation has a rather symmetric structure with a dip in the center, indicating that the phase difference between the bound-state pulses is roughly π as predicted theoretically in [32], [33]. Compared with that in Fig. 2(b), the autocorrelation trace on Fig. 3(b) has two new sidebands that

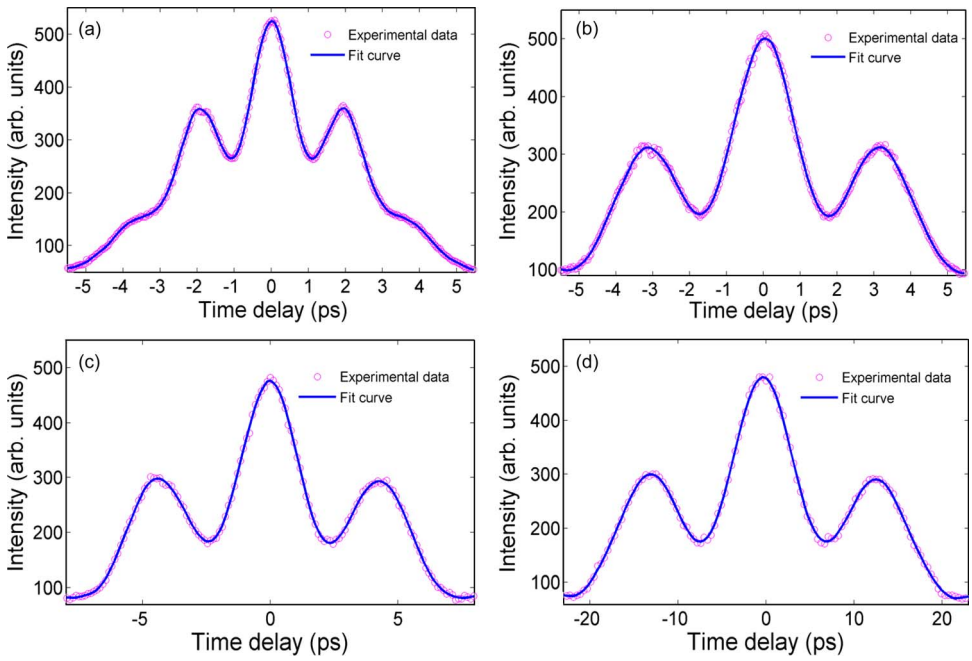

Fig. 4. Autocorrelation traces of bound-state pulses via (a) 22, (b) 42, (c) 62, and (d) 202 m of the standard SMF.

are separated from the central peak by ~2.2 ps. The height of side peak is half of the main peak, which means that the two bound-state pulses are identical. The FWHM of each pulse is ~1.3 ps if the Gaussian profile is assumed, which agrees well with the result mentioned above. Thus, the pulse separation between the two pulses is 1.7 times of the pulse duration. Such a small separation indicates that there should be an attractive or repulsive force exerted on the respective pulse due to direct pulse interaction [32]. According to the FT theory, the 2.2-ps separation between the two identical pulses in the temporal domain would lead to the 3.6-nm peak-to-peak spacing in the spectrum domain (considering that the center wavelength is 1567 nm), which is rather coincident with the experimental result in Fig. 3(a).

Further increasing the pump power P to 550 mW, the operation of bound-state pulses maintains. No obvious difference is observed except the increased intensity. As a consequence, we conclude that once the bound-state is formed, slightly changing the laser operation conditions (e.g., the pump strength and the orientations of the PCs) does not change the pulse duration or the pulse separation but influences the peak power. The value seems fixed in every self-started mode-locking state for our laser, indicating that the pulses are tightly bound and the phase difference between the bound-state pulses is stable [31], [35]. Conceptually, the formation of stable bound-state can be described by the following two steps. First, similar to multiple pulses operation in passively mode-locked fiber laser, pulse splitting can occur as a result of the pulse energy quantization [34]. Second, the two pulses would begin to affect each other when they are so close that their tails overlap [1]. Because of the relatively close pulse separation in the system, each of the split pulses should experience the balanced attractive or repulsive forces simultaneously when propagating along the cavity due to direct pulses interaction, which gives rise to stable bound-state pulses. As a consequence, bound-state pulses formed in the system have an oscillating tail [31]. Therefore, our experimental results are completely different from the report in [36], in which the dispersive waves play an essential role in the long-range interaction among the bound solitons.

The propagation dynamics of bound-state pulses are investigated by utilizing SMF with different lengths. Fig. 4(a)–(d) show the autocorrelation traces after passing through 22, 42, 62, and 202 m of SMF, respectively. The intensities of side peaks are always half of the main peak, indicating that the two pulses have equal peak power during propagation. More details about pulse evolution as a

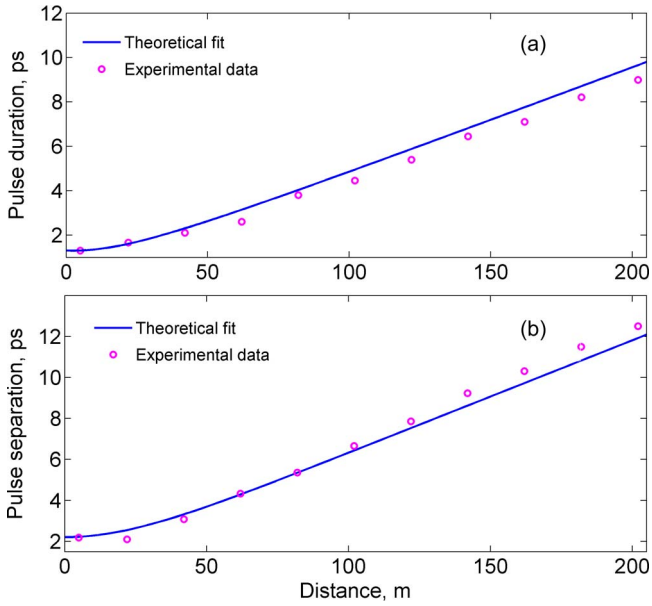

Fig. 5. Evolution of (a) pulse duration and (b) pulse separation of bound-state pulses with respect to the transmission distance of the extracavity SMF.

function of propagation length can be obtained in Fig. 5. One can see that the pulse duration and separation vary slowly under a short transmission fiber (less than 22 m) and increase approximately linearly with larger fiber length (22–202 m). The pulse duration and separation are increased by a factor of ~7 and ~5.7, respectively, after the pulse pair propagates through 202-m SMF.

We have also theoretical studied propagation of the bound-state pulses in SMF. When the pulse passing through the extracavity SMF, the pulse duration T_z is expressed as [1]

$$T_z = 2\ln(1+\sqrt{2})T_0\left[(1+z\beta_2 C/T_0^2)^2+(z\beta_2/T_0^2)^2\right]^{1/2}. \quad (1)$$

The chirp parameter also changes from C to C_1 after propagation through distance z such that [1]

$$C_1(z) = C + (1+C^2)(\beta_2 z/T_0^2). \quad (2)$$

Based on the perturbed nonlinear Schrödinger equation theory in [1], the relative separation q between the bound-state pulses can be described as

$$q = q_0 + 1/2\ln\left[\cosh^2(2\xi e^{-q_0}\sin\psi_0)+\cos^2(2\xi e^{-q_0}\cos\psi_0)-1\right]. \quad (3)$$

Here, β_2 is the group velocity dispersion (GVD) of SMF, and T_0 is the half-width ($1/e$-intensity). C is the initial chirp parameter, which is expressed by $C=\sqrt{(\Delta w T_0)^2-1}$, where Δw is the spectral half-width (at $1/e$-intensity point). q_0 and ψ_0 are the initial values of relative separation and relative phase. The variables z and $\xi = z/L_D$ ($L_D = T_0^2/|\beta_2|$) represent the propagation distance and the normalized distance, respectively.

For the modeling, we use the following parameters for our simulations for possibly matching the experimental conditions: $\beta_2 = -0.02$ ps^2/m for the SMF, $T_0 = 0.74$ ps, $C = -0.1$, $\Delta w = 1.36$ THz, $\theta = 2\psi_0 = \pi$ for the initial phase difference, and $2q_0 = 2.2$ ps for the initial separation between the two pulses, respectively.

The solid curve in Fig. 5(a) shows the evolution of pulse duration as a function of distance. It is seen that the pulse duration changes slightly at first while almost increases linearly for longer distance, which is in good agreement with the experimental observations. As dispersion-induced chirp are added to the initial chirp for $\beta_2 C > 0$, the pulse broadens monotonically with fiber length (z)

at a rate faster than that of an unchirped pulse. We have found that the optical spectrum almost maintains it profile after propagation through SMF, indicating that the nonlinear effects play a relatively minor role. Based on the results, we conclude that the evolution of pulse duration is governed by GVD of SMF.

The evolution of the separation along propagation distance is denoted by solid curve in Fig. 5(b). It is found that, with the increase of distance, the pulse separation varies slowly at first while almost increase linearly for longer SMF. One can see that the simulations have well reproduced the experimental results. Depending on the initial value of phase difference θ, two pulses may attract or repel each other. For $\theta = \pi$, q is larger than q_0 and increases monotonically with ξ. This is interpreted as a nonlinearity-induced repulsive force between the two pulses. Here, $\theta = \pi$ corresponds to two pulses that are initially out of phase. Our results indicate that the two pulses with different phase can form a bound-state pulse in figure-eight fiber laser.

4. Conclusion

The generation and propagation of bound-state pulses in a passively mode-locked figure-eight laser is investigated experimentally and theoretically. The experimental results show that the proposed laser operates on the single-pulse state when the pump power P is less than 9 mW, whereas it delivers the bound-state pulses for $P > 9$ mW. The pulse duration and the separation of pulse pair in the cavity are about 1.3 and 2.2 ps, respectively. The experiments demonstrate that both the pulse duration and the separation increase approximately linearly along the extracavity SMF. After the pulse pair propagates via the standard SMF with the distance of 202 m, the pulse duration and separation are increased by a factor of $\sim$7 and $\sim$5.7, respectively. The theoretical results well confirm the experimental observations.

References

[1] G. P. Agrawal, *Nonlinear Fiber Optics,* 4th ed. Boston, MA: Academic, 2007.
[2] X. Liu, X. Tang, F. Lu, J. Ng, X. Zhou, and C. Lu, "Stable and uniform dual-wavelength erbium-doped fiber laser based on fiber Bragg gratings and photonic crystal fiber," *Opt. Exp.*, vol. 13, no. 1, pp. 142–147, Jan. 2005.
[3] G. Martel, C. Chédot, V. Réglier, A. Hideur, B. Ortaç, and P. Grelu, "On the possibility of observing bound soliton pairs in a wave-breaking-free mode-locked fiber laser," *Opt. Lett.*, vol. 32, no. 4, pp. 343–345, Feb. 2007.
[4] S. Chouli and P. Grelu, "Soliton rains in a fiber laser: An experimental study," *Phys. Rev. A*, vol. 81, no. 6, pp. 063829-1–063829-10, Jun. 2010.
[5] L. R. Wang, X. M. Liu, Y. K. Gong, D. Mao, and L. N. Duan, "Observations of four types of pulses in a fiber laser with large net-normal dispersion," *Opt. Exp.*, vol. 19, no. 8, pp. 7616–7624, Apr. 2011.
[6] W. Chang, A. Ankiewicz, J. M. Soto-Crespo, and N. Akhmediev, "Dissipative soliton resonances," *Phys. Rev. A*, vol. 78, no. 2, pp. 023830-1–023830-9, Aug. 2008.
[7] X. Liu, "Mechanism of high-energy pulse generation without wave breaking in mode-locked fiber lasers," *Phys. Rev. A*, vol. 82, no. 5, pp. 053808-1–053808-5, Nov. 2010.
[8] A. Zavyalov, R. Iliew, O. Egorov, and F. Lederer, "Discrete family of dissipative soliton pairs in mode-locked fiber lasers," *Phys. Rev. A*, vol. 79, no. 5, pp. 053841-1–053841-10, May 2009.
[9] Z. X. Zhang and G. X. Dai, "All-normal-dispersion dissipative soliton Ytterbium fiber laser without dispersion compensation and additional filter," *IEEE Photon. J*, vol. 3, no. 6, pp. 1023–1029, Dec. 2011.
[10] D. Mao, X. M. Liu, L. R. Wang, X. H. Hu, and H. Lu, "Partially polarized wave-breaking-free dissipative solitons with super-broad spectrum in a mode-locked fiber laser," *Laser Phys. Lett.*, vol. 8, no. 2, pp. 134–138, Feb. 2011.
[11] L. R. Wang, X. M. Liu, and Y. K. Gong, "Giant-chirp oscillator for ultra-large net-normal-dispersion fiber lasers," *Laser Phys. Lett.*, vol. 7, no. 1, pp. 63–67, Jan. 2010.
[12] C. M. Ouyang, P. P. Shum, K. Wu, J. H. Wong, X. Wu, H. Q. Lam, and S. Aditya, "Dissipative soliton (12 nJ) from an all-fiber passively mode-locked laser with large normal dispersion," *IEEE Photon. J.*, vol. 3, no. 5, pp. 881–887, Oct. 2011.
[13] X. M. Liu, "Interaction and motion of solitons in passively-mode-locked fiber lasers," *Phys. Rev. A*, vol. 84, no. 5, pp. 053828-1–053828-6, Nov. 2011.
[14] X. M. Liu, "Soliton formation and evolution in passively-mode-locked lasers with ultralong anomalous-dispersion fibers," *Phys. Rev. A*, vol. 84, no. 2, pp. 023835-1–023835-7, Aug. 2011.
[15] X. M. Liu, T. Wang, C. Shu, L. R. Wang, A. Lin, K. Q. Lu, T. Y. Zhang, and W. Zhao, "Passively harmonic mode-locked erbium-doped fiber soliton laser with a nonlinear polarization rotation," *Laser Phys.*, vol. 18, no. 11, pp. 1357–1361, Nov. 2008.
[16] H. Zhang, D. Y. Tang, L. M. Zhao, X. Wu, and H. Y. Tam, "Dissipative vector solitons in a dispersion-managed cavity fiber laser with net positive cavity dispersion," *Opt. Exp.*, vol. 17, no. 2, pp. 455–460, Jan. 2009.
[17] H. Zhang, D. Y. Tang, L. M. Zhao, and R. J. Knize, "Vector dark domain wall solitons in a fiber ring laser," *Opt. Exp.*, vol. 18, no. 5, pp. 4428–4433, Mar. 2010.

[18] P. Grelu, F. Belhache, F. Gutty, and J. M. Soto-Crespo, "Phase-locked soliton pairs in a stretched-pulse fiber laser," *Opt. Lett.*, vol. 27, no. 11, pp. 966–968, Jun. 2002.
[19] W.-W. Hsiang, C.-Y. Lin, and Y. Lai, "Stable new bound soliton pairs in a 10 GHz hybrid frequency modulation mode-locked Er-fiber laser," *Opt. Lett.*, vol. 31, no. 11, pp. 1627–1629, Jun. 2006.
[20] N. H. Seong and D. Y. Kim, "Experimental observation of stable bound solitons in a figure-eight fiber laser," *Opt. Lett.*, vol. 27, no. 15, pp. 1321–1323, Aug. 2002.
[21] M. Olivier, V. Roy, and M. Piché, "Third-order dispersion and bound states of pulses in a fiber laser," *Opt. Lett.*, vol. 31, no. 5, pp. 580–582, Mar. 2006.
[22] P. Grelu, W. Chang, A. Ankiewicz, J. M. Soto-Crespo, and N. Akhmediev, "Dissipative soliton resonance as a guideline for high-energy pulse laser oscillators," *J. Opt. Soc. Amer. B*, vol. 27, no. 11, pp. 2336–2341, Nov. 2010.
[23] L. N. Duan, X. M. Liu, D. Mao, L. R. Wang, and G. X. Wang, "Experimental observation of dissipative soliton resonance in an anomalous-dispersion fiber laser," *Opt. Exp.*, vol. 20, no. 1, pp. 265–270, Jan. 2012.
[24] X. M. Liu, "Pulse evolution without wave breaking in a strongly dissipative-dispersive laser system," *Phys. Rev. A*, vol. 81, no. 5, pp. 053819-1–053819-6, May 2010.
[25] X. M. Liu, "Dynamic evolution of temporal dissipative-soliton molecules in large normal path-averaged dispersion fiber lasers," *Phys. Rev. A*, vol. 82, no. 6, pp. 063834-1–063834-6, Dec. 2010.
[26] B. Ortaç, A. Hideur, T. Chartier, M. Brunel, P. Grelu, H. Leblond, and F. Sanchez, "Generation of bound states of three ultrashort pulses with a passively mode-locked high-power Yb-doped double-clad fiber laser," *IEEE Photon. Technol. Lett.*, vol. 16, no. 5, pp. 1274–1276, May 2004.
[27] N. N. Akhmediev, A. Ankiewicz, and J. M. Soto-Crespo, "Multisoliton solutions of the complex Ginzburg-Landau equation," *Phys. Rev. Lett.*, vol. 79, no. 21, pp. 4047–4051, Nov. 1997.
[28] M. Salhi, A. Haboucha, H. Leblond, and F. Sanchez, "Theoretical study of figure-eight all-fiber laser," *Phys. Rev. A*, vol. 77, no. 3, pp. 033828-1–033828-9, Mar. 2008.
[29] M. Stratmann, T. Pagel, and F. Mitschke, "Experimental observation of temporal soliton molecules," *Phys. Rev. Lett.*, vol. 95, no. 14, pp. 143902-1–143902-4, Sep. 2005.
[30] W. Chang, N. Akhmediev, and S. Wabnitz, "Effect of an external periodic potential on pairs of dissipative solitons," *Phys. Rev. A*, vol. 80, no. 1, pp. 013815-1–013815-5, Jul. 2009.
[31] D. Y. Tang, B. Zhao, L. M. Zhao, and H. Y. Tam, "Soliton interaction in a fiber ring laser," *Phys. Rev. E*, vol. 72, no. 1, pp. 016616-1–016616-10, Jul. 2005.
[32] J. M. Soto-Crespo, N. Akhmediev, P. Grelu, and F. Belhache, "Quantized separations of phase-locked soliton pairs in fiber lasers," *Opt. Lett.*, vol. 28, no. 19, pp. 1757–1759, Oct. 2003.
[33] J. M. Soto-Crespo and N. Akhmediev, "Composite solitons and two-pulse generation in passively mode-locked lasers modeled by the complex quintic Swift-Hohenberg equation," *Phys. Rev. E*, vol. 66, no. 6, pp. 066610-1–066610-10, Dec. 2002.
[34] X. M. Liu, "Hysteresis phenomena and multipulse formation of a dissipative system in a passively mode-locked fiber laser," *Phys. Rev. A*, vol. 81, no. 2, pp. 023811-1–023811-6, Feb. 2010.
[35] B. A. Malomed, "Bound states of envelope solitons," *Phys. Rev. E*, vol. 47, no. 4, pp. 2874–2880, Apr. 1993.
[36] D. Y. Tang, B. Zhao, D. Y. Shen, and C. Lu, "Bound-soliton fiber laser," *Phys. Rev. A*, vol. 66, no. 3, pp. 033806-1–033806-6, Sep. 2002.